ACS Medicinal Chemistry Letters
Cite This: ACS Med. Chem. Lett. XXXX, XXX, XXX−XXX
Letter
pubs.acs.org/acsmedchemlett

Discovery of Orally Active Hydroxyethylamine Based SPPL2a Inhibitors

Juraj Velcicky,*[,†] Casey J. N. Mathison,[§] Victor Nikulin,[§] Daniel Pflieger,[†] Robert Epple,[§] Mihai Azimioara,[§] Christopher Cow,[§] Pierre-Yves Michellys,[§] Pascal Rigollier,[†] Daniel R. Beisner,[§] Ursula Bodendorf,[‡] Danilo Guerini,[‡] Bo Liu,[§] Ben Wen,[§] Samantha Zaharevitz,[§] and Trixi Brandl[†]

[†]Global Discovery Chemistry, and [‡]Autoimmunity Transplantation Inflammation, Novartis Institutes for BioMedical Research, CH-4002 Basel, Switzerland

[§]The Genomics Institute of the Novartis Research Foundation, 10675 John Jay Hopkins Drive, San Diego, California 92121, United States

Supporting Information

ABSTRACT: SPPL2a (Signal Peptide Peptidase Like 2a) is an intramembrane aspartyl protease engaged in the function of B-cells and dendritic cells. Despite being an attractive target for modulation of the immune system, selective SPPL2a inhibitors are barely described in the literature. Recently, we have disclosed a selective, small molecular weight agent SPL-707 which confirmed that pharmacological inhibition of SPPL2a leads to the accumulation of its substrate CD74/p8 and as a consequence to a reduction in the number of B-cells as well as myeloid dendritic cells in mice. In this paper we describe the discovery of novel hydroxyethylamine based SPPL2a inhibitors. Starting from a rather lipophilic screening hit, several iterative optimization cycles allowed for its transformation into a highly potent and selective compound **15** (**SPL-410**) which inhibited *in vivo* CD74/p8 fragment processing in mice at 10 mg/kg oral dose.

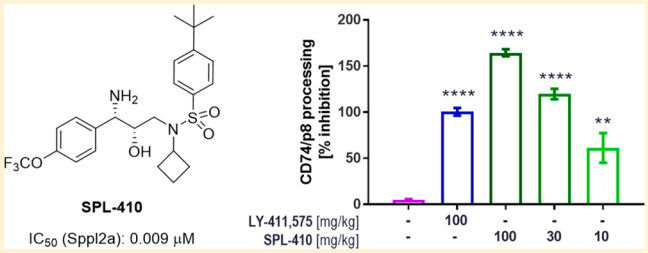

KEYWORDS: *SPPL2a, CD74, hydroxyethylamine, sulfonamide, inhibitor, oral activity*

The immune system is a powerful host defense mechanism specializing in antigen recognition. As a consequence, it is of a vital importance for the immune system to properly learn to distinguish between foreign and self-antigens in order to prevent destruction of the body's own tissue.[1] Loss of tolerance to self-antigens leads to pathological conditions which are manifested as autoimmune diseases.[2] Drugs reducing the antigen presenting capacity of the immune system, for example B-cell depleting agents such as rituximab (anti-CD20 antibody), are therapeutically beneficial in the treatment of rheumatoid arthritis, systemic lupus erythematosus, multiple sclerosis, or graft versus host disease.[3] The successful use of B-cell depleting agents in the control of autoimmune diseases fueled the search for low molecular weight agents reducing the number of antigen presenting cells (APCs) and/or their antigen presenting capacity.[4] SPPL2a (Signal Peptide Peptidase Like 2a) is an intramembrane aspartyl protease[5] shown to be engaged in the function of B-cells[6−8] and conventional dendritic cells[6−9] in mice and humans. The mechanism how SPPL2a inhibition leads to reduction in the number of APCs is not yet fully understood. However, it could be shown that among several type II transmembrane proteins, SPPL2a is involved in the intramembrane-cleavage of the membrane-bound *N*-terminal p8 fragment (NTF) of CD74.[10] Major histocompatibility complex class II (MHC II) requires CD74 for its transport from the endoplasmic reticulum to the late endosome for antigen binding.[11] Once arrived in the endosome, the membrane anchored CD74 undergoes a rapid cathepsin mediated degradation. Subsequently, the released MHC II binds endosomaly processed antigens and presents them on the cell surface whereas the remaining membrane bound CD74/p8 NTF is cleared from the membrane by SPPL2a. The B-cell receptor (BCR) is important for the survival of the developing B-cells.[12] It could be shown that processing of CD74/p8 NTF by SPPL2a is required for appropriate levels of tonic BCR signaling to promote B cell maturation.[13] In line with the studies using SPPL2a deficient mice, the SPPL2a low molecular weight inhibitor SPL-707 (Figure 1) demonstrated that pharmacological inhibition of SPPL2a also prevents CD74/p8 NTF processing and as a consequence leads to a reduction in the number of B-cells and myeloid dendritic cells.[14] As a part of our continuous effort toward identification of SPPL2a inhibitors, herein we describe the discovery of a novel, potentially active site binding scaffold.

Whereas the potent and selective SPPL2a inhibitor SPL-707[14] could be developed starting from the known

Received: February 4, 2019
Accepted: May 16, 2019

DOI: 10.1021/acsmedchemlett.9b00044
ACS Med. Chem. Lett. XXXX, XXX, XXX−XXX

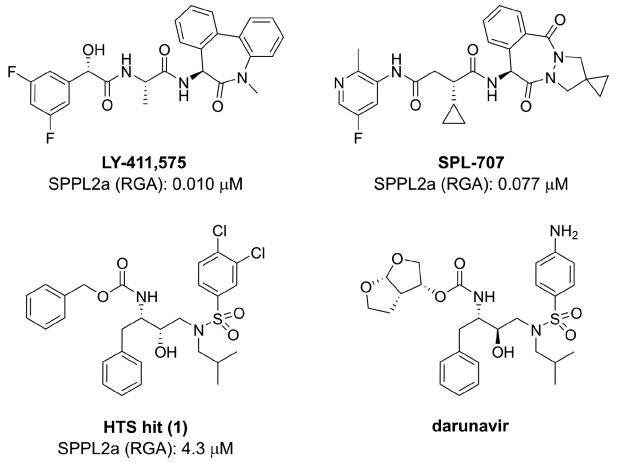

Figure 1. Structures of the known SPPL2a inhibitors LY-411,575 and SPL-707, HTS hit **1**, and HIV protease inhibitor darunavir.

γ-secretase inhibitor LY-411,575, compound **1** (Figure 1) was discovered as a hit in the high throughput screening of the Novartis compound archive.[15] Despite the rather high lipophilicity of **1**, the scaffold appealed to us because of its structural similarity to the marketed HIV-protease inhibitors such as, for example, darunavir (Figure 1).[16] In addition, the hydroxyethylamine (HEA) fragment present in **1** is a known transition state binding motif[17] which apart from HIV protease,[16] has successfully been applied in the design of agents inhibiting other aspartyl proteases such as BACE-1,[18] cathepsin D,[19] and plasmepsin.[20]

Whereas for most of the HEA-containing inhibitors it is beneficial to keep a substituent at the amine (usually carbamates such as the bis-THF moiety in darunavir), this was not the case for SPPL2a since the Cbz group removal led to a more potent while less lipophilic derivative **2** (Table 1). Additional truncation (benzyl to phenyl group in **3**) further enhanced the potency and at the same time also solubility. Interestingly, compound **3** displayed a high selectivity against other aspartyl proteases such as BACE 1 and 2, cathepsin D and E, as well as renin (all >100 μM) and even against the closely related γ-secretase (4.8 μM) and SPP (8.1 μM) (Table 2). Therefore, the next round of optimization started with **3** and focused on derivatization of the sulfonamide *N*-substituent (Table 2).

Due to a relatively high intrinsic clearance of compound **3**, as assessed in mouse liver microsomes, addition of polar substituents at this position was tested for potential reduction in clearance. While hydroxy-derivative **4** led indeed to an improved intrinsic clearance, a drop in SPPL2a potency was observed. On the other hand, the oxo-derivative **5** did essentially keep the same potency but surprisingly it was even more rapidly metabolized than **3** (Table 2). While larger lipophilic substituents had no advantage in terms of potency and clearance as illustrated by the Bn-analog **6**, α-branched aliphatic and especially cyclic groups appeared to be more optimal at this position (Table 2). For example, cyclobutyl analog **7** showed not only improved potency but also reduced clearance compared to **3**. Larger rings such as cycloheptyl in **8** further boosted the potency as well as selectivity but led to increased lipophilicity (log $D_{7.4}$ 4.0 for **8** vs 2.8 for **7**) and hence also clearance. Adding an oxo-substituent to the cyclobutyl group resulted in a more polar and metabolically more stable oxetane analog **9** being again less tolerated by

Table 1. Initial Round of Optimization

Compd	Structure	hSPPL2a[a] [μM]	$logD_{7.4}$[b] (clogP)	Solubility[c] [g/L]
1	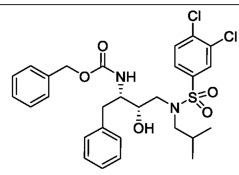	4.3	>4.6 (7.0)	< 0.002
2	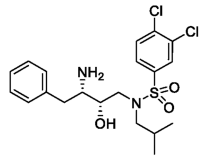	0.86	3.1 (4.7)	< 0.002
3	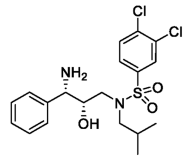	0.20	3.1 (4.3)	0.034

[a]IC_{50} determined as a mean ($n \geq 3$) in HEK293 cells cotransfected with TNFα-NTF/VP16-GAL4 fusion and human SPPL2a (RGA). [b]log $D_{7.4}$ was determined at pH 7.4 by a rapid-throughput octanol-buffer lipophilicity measurement based on 96-well shake flask equilibrium and LC/MS/MS analysis. [c]Equilibrium solubility determined by saturation shake flask method at pH 6.8 using DMSO solution.[21]

SPPL2a. In addition, further branching to tertiary groups, as exemplified by derivative **10**, was also not favored by SPPL2a. Based on the balanced SPPL2a potency and clearance, the cyclobutyl group was kept for further optimization of the scaffold.

Exploration of the arylsulfonyl substituent revealed this part of the molecule to be important for gaining potency against SPPL2a (Table 3). While bulky lipophilic substituents like tetramethyltetrahydronaphthalene (**11**) improved the potency, polar substituents such as, for example, benzothiazole (**12**) were not well accepted by SPPL2a. Interestingly, a single *t*-Bu group at the phenyl ring was found to be sufficient to keep high SPPL2a potency while the clearance of these mono-*t*-Bu analogs was dependent on its position, with *m*-derivative **13** being metabolized quicker than its *p*-analog **14** (Table 3). Further decoration of **14** by the trifluoromethoxy group at the *para*-position of the unsubstituted phenyl ring led to compound **15** (**SPL-410**), a highly potent and selective SPPL2a inhibitor.

The potent inhibition of SPPL2a by compound **15**, as measured in the reporter gene assay (RGA), could also be confirmed using an orthogonal, imaging based SPPL2a assay (high content imaging assay; HCA).[14,15] Both human and mouse SPPL2a was inhibited with high potency (IC_{50} of 0.004 μM and 0.005 μM) in the respective HCA. In addition, the processing of the endogenous substrate, CD74/p8 NTF, was inhibited by **15** with an IC_{50} of 0.15 μM as assessed in the mouse B cell line A20 by a quantitative Western Blot assay (Supporting Information Figure S1). Moreover, compound **15** proved to be selective against closely related human aspartyl proteases such as SPP (0.65 μM) and γ-secretase (1.3 μM) (Table 3) as well as SPPL2b (0.27 μM in HCA). Cellular data

DOI: 10.1021/acsmedchemlett.9b00044
ACS Med. Chem. Lett. XXXX, XXX, XXX−XXX

Table 2. SAR around Sulfonamide *N*-Substituent

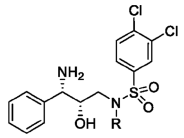

Compd	R	hSPPL2a[a] [μM]	γ-secretase[b] [μM]	hSPP[c] [μM]	mouse Clint[d] [μL/min/kg]
3		0.20	4.8	8.1	154
4		0.91	>10	>32	84
5		0.35	5.9		335
6		0.62	3.4	3.2	246
7		0.088	5.1	3.5	102
8		0.015	2.1	3.9	192
9		1.5	>10	26	46
10		0.90	6.4		

IC_{50} determined as a mean ($n \geq 3$) in [a]HEK293 cells cotransfected with TNFα-NTF/VP16-GAL4 fusion and human SPPL2a (RGA); [b]HEK293 cells cotransfected with Notch1-VP16-GAL4 fusion (RGA); [c]stable U-2 OS cell lines expressing human SPP constitutively and an inducible EGFP-labeled EnvSigSeq-SEAP fusion protein substrate (HCA).[14,15] [d]Intrinsic clearance determined by the disappearance of the parent compound from the reaction media using mouse liver microsomes.[22] Dashed lines represent the attachment points of substituents to the scaffold.

Table 3. Optimization of the Aryl Substituent

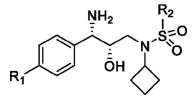

Compd	R_1	R_2	hSPPL2a[a] [μM]	γ-secretase[b] [μM]	hSPP[c] [μM]	mouse Clint[d] [μL/min/kg]
7	H		0.088	5.1	1.8	102
11	H	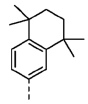	0.013	1.8	1.5	242
12	H		0.84	>10		
13	H		0.007	3.7	2.0	338
14	H	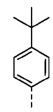	0.025	3.7	3.3	127
15	CF_3O	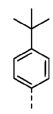	0.009	1.3	0.65	109

IC_{50} determined as a mean ($n \geq 3$) in [a]HEK293 cells cotransfected with TNFα-NTF/VP16-GAL4 fusion and human SPPL2a (RGA); [b]HEK293 cells cotransfected with Notch1-VP16-GAL4 fusion (RGA); [c]stable U-2 OS cell lines expressing human SPP constitutively and an inducible EGFP-labeled EnvSigSeq-SEAP fusion protein substrate (HCA).[14,15] [d]Intrinsic clearance determined by the disappearance of the parent compound from the reaction media using mouse liver microsomes.[22] Dashed lines represent the attachment points of substituents to the scaffold.

for different assay formats and enzymes are summarized in Supporting Information Table S1.

Interestingly, despite increased lipophilicity compared to its analog **14**, compound **15** displayed a slightly improved metabolic stability in mouse liver microsomes (Table 3). Notably, such a positive effect of the trifluoromethoxy group on clearance seems to be rather specific for this compound since it usually led to an opposite effect within this series, it means to a lower metabolic stability of the corresponding trifluoromethoxy analogs. In order to determine the *in vivo* clearance as well as other pharmacokinetic parameters of this promising candidate, mice were dosed with **15** at 5 mg/kg i.v. and 20 mg/kg p.o. (Figure 2A). Whereas the compound showed moderate *in vivo* clearance (41 mL/min/kg), a rather long $t_{1/2}$ of 5.0 h was observed being driven by its high volume of distribution (12.3 L/kg). The oral bioavalability (35%) and oral exposure (282 h*nM AUC dose normalized) were moderate but suitable for oral dosing.

In vivo inhibition of SPPL2a by compound **15** was evaluated by treating mice with a 10, 30, and 100 mg/kg single p.o. dose of **15** and measuring the accumulation of CD74/p8 NTF 4 h later in splenocyte lysates[14] (Figure 2B,C and Supporting Information Figure S2). In this mechanistic model, **15** showed a dose-linear exposure in plasma and spleen and a nice dose−response for CD74/p8 NTF accumulation in splenocytes. In addition, **15** achieved a higher efficacy than our benchmark compound LY-411,575 at the same dose (Figure 2B).

Although a relatively high exposure of **15** was reached in spleen at 10 mg/kg dose (Figure 2C), no full efficacy was observed at this dose. The reason for this might be a poor activity (4.0 μM) of compound **15** as measured in a mouse whole blood assay assessing accumulation of the CD74/p8 NTF (Supporting Information Table S1 and Figure S3). Hence, the 6.0 μM spleen levels reached at 4 h with the 10 mg/kg dose appear rather low for getting the full inhibition of SPPL2a. The 30-fold drop in potency seen in the whole blood assay most probably reflects the very high plasma protein

DOI: 10.1021/acsmedchemlett.9b00044
ACS Med. Chem. Lett. XXXX, XXX, XXX−XXX

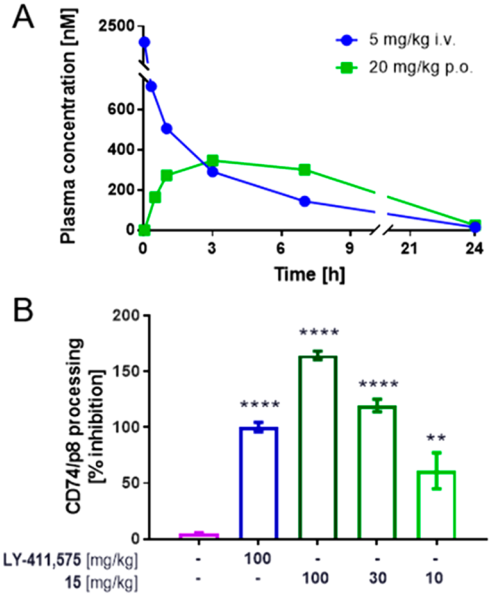

C

Dose [mg/kg]	Plasma conc. [μM]	Spleen conc. [μM]
100	1.17 ± 0.61	53.3 ± 19.8
30	0.25 ± 0.06	12.7 ± 2.6
10	0.12 ± 0.02	6.0 ± 2.2

Figure 2. (A) Pharmacokinetic profile of compound **15** determined as a mean plasma concentration of three animals (Balb\c mice) after dosing the compound using a PEG300/D5W (3:1) formulation for i.v. and p.o. application. (B) Inhibition of CD74/p8 NTF processing in mice after oral treatment with **15**. Mice received single oral doses of 100 mg/kg LY-411,575 or 10, 30, and 100 mg/kg **15** using PEG300/D5W (3:1) formulation. Four h after dosing, inhibition of SPPL2a *in vivo* was assessed by measuring CD74/p8 NTF accumulation in splenocyte lysates by Western blot analysis with an antimouse CD74 antibody. Relative quantification of the p8 bands is shown, and the reference sample with LY-411,575 was set arbitrarily as 100%. (C) Total plasma and spleen concentrations (means ± SEM) of **15** at termination of the study 4 h after dosing. Statistics are one-way ANOVA followed by Dunnett's test compared to matched vehicle group: * $p \leq 0.05$; ** $p \leq 0.01$; *** $p \leq 0.001$; **** $p \leq 0.0001$.

binding (PPB, >99% across species) determined for **15**, being the case also for other compounds within the series. Therefore, further work focusing on lowering the PPB will be necessary for this scaffold for improvement of its potency in whole blood and hence, *in vivo*.

The described compounds were prepared as illustrated by synthesis of **15** (Scheme 1). The required trifluoromethoxy building block **18** was obtained in five steps starting from the known allylic alcohol **17**[23] in analogy to the procedure described for preparation of the unsubstituted azidoepoxide **20**.[24] Base catalyzed epoxide opening[25] in **18** was achieved using sulfonamide **16** that was prepared in a single step from the corresponding sulfonyl chloride and cyclobutylamine. Reduction of the azide group in **19** provided compound **15** in good overall yield. The hydroxylamine analog **5** was assembled in a similar manner but starting from the Boc-protected aminoepoxide **21**,[26] and the Bn-analog **2** was prepared from **22**[27] (Scheme 1). Attachment of the Cbz-group to the primary amine in **2** provided compound **1**.

Scheme 1. Synthesis of Compound 15 and Its Analogs[a]

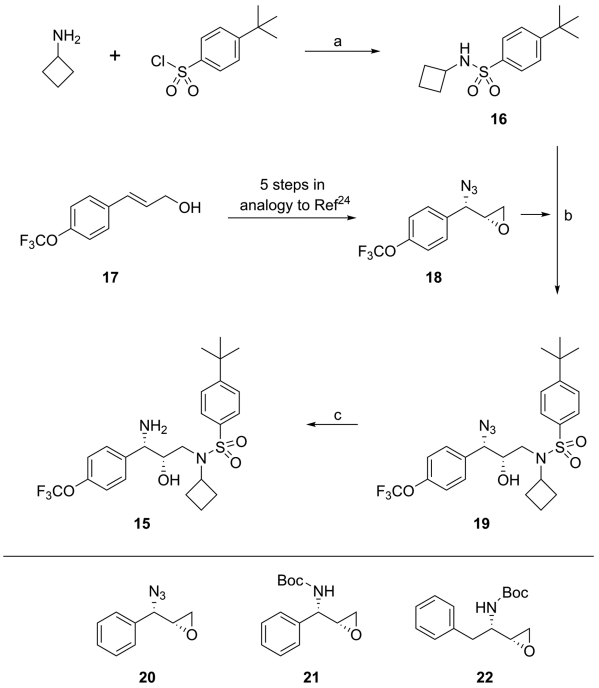

[a]*Reagents and conditions:* (a) DIPEA, CH_2Cl_2, 23 °C, 16 h (85%); (b) DBU, *i*-PrOH, 85 °C, 16 h (69%); (c) Me_3P, THF/H_2O, 23 °C, 3 h (71%).

In summary, in this paper we have described our discovery of a novel HEA-containing SPPL2a scaffold derived from an HTS campaign. Without any available structural data it remains uncertain how these inhibitors bind into SPPL2a. However, thanks to the present HEA, a known aspartyl protease transition state binding motif, it may be assumed that the described SPPL2a inhibitors bind into the active site of SPPL2a. The hit **1** could be optimized into a selective and highly potent SPPL2a inhibitor **15** (**SPL-410**) with decent oral exposure in mice. In the mechanistic mouse model, this compound displayed a significant inhibition of CD74/p8 NTF processing even at 10 mg/kg oral dose. The main drawback of this series is the loss of potency of CD74/p8 NTF processing in the presence of whole blood which may be a result of the high PPB being typically >99% across species. This parameter is most probably driven by the high lipophilicity of this scaffold which, however, seems to be dictated by the SPPL2a binding site. Therefore, we believe that more polar analogs may help to address this issue and potentially allow for improved potency in the whole blood assay and *in vivo* inhibition of SPPL2a at lower doses.

■ ASSOCIATED CONTENT

Supporting Information

The Supporting Information is available free of charge on the ACS Publications website at DOI: 10.1021/acsmedchemlett.9b00044.

Description of *in vitro* assays, pharmacokinetic measurements, synthesis procedures and characterization data for all compounds, and UPLC and NMR charts for compound **15** (PDF)

DOI: 10.1021/acsmedchemlett.9b00044
ACS Med. Chem. Lett. XXXX, XXX, XXX−XXX

AUTHOR INFORMATION

Corresponding Author

*Juraj Velcicky, e-mail: juraj.velcicky@novartis.com.

ORCID

Juraj Velcicky: 0000-0001-6564-1448

Present Address

M.A.: Plexium, Inc., 4204 Sorrento Valley Boulevard, Suite A, San Diego, CA 92121, USA. D.R.B.: Vividion Therapeutics, 5820 Nancy Ridge Dr., San Diego, CA 92121, USA.

Notes

The authors declare no competing financial interest.

ACKNOWLEDGMENTS

The authors would like to thank Stephane Rodde and Damien Hubert for the physicochemical measurements and Corinne Marx for HRMS measurements.

ABBREVIATIONS

BACE, β-secretase; DBU, 1,8-diazabicyclo[5.4.0]undec-7-en; DIPEA, ethyldiisopropyl amine; D5W, 5% dextrose in water; EGFP, green fluorescent protein; EnvSigSeq, hepatitis C virus envelope protein signal peptide; GAL4, regulatory protein galactose 4; HCA, high content imaging assay; RGA, reporter gene assay; SEAP, secreted embryonic alkaline phosphatase; SPP, signal peptide peptidase; TNFα, tumor necrosis factor alpha; VP16, virus protein 16.

REFERENCES

(1) Janeway, C. A.; Travers, P.; Walport, M.; Shlomchik, M. *Immunobiology: The Immune System in Health and Disease*, 6th ed.; Garland Science, 2004.

(2) Roghanian, A. https://www.immunology.org/public-information/bitesized-immunology/immune-dysfunction/b-cell-mediated-disease.

(3) Gürcan, H. M.; Keskin, D. B.; Stern, J. N. H.; Nitzberg, M. A.; Shekhani, H.; Ahmed, A. R. A review of the current use of rituximab in autoimmune diseases. *Int. Immunopharmacol.* **2009**, *9*, 10−25.

(4) Franks, S. E.; Getahun, A.; Hogarth, P. M.; Cambier, J. C. Targeting B cells in treatment of autoimmunity. *Curr. Opin. Immunol.* **2016**, *43*, 39−45.

(5) Weihofen, A.; Binns, K.; Lemberg, M. K.; Ashman, K.; Martoglio, B. Identification of signal peptide peptidase, a presenilin-type aspartic protease. *Science* **2002**, *296*, 2215−2218.

(6) Beisner, D. R.; Langerak, P.; Parker, A. E.; Dahlberg, C.; Otero, F. J.; Sutton, S. E.; Poirot, L.; Barnes, W.; Young, M. A.; Niessen, S.; Wiltshire, T.; Bodendorf, U.; Martoglio, B.; Cravatt, B.; Cooke, M. P. The intramembrane protease SPPL2a is required for B cell and DC development and survival via cleavage of the invariant chain. *J. Exp. Med.* **2013**, *210*, 23−30.

(7) Bergmann, H.; Yabas, M.; Short, A.; Miosge, L.; Barthel, N.; Teh, C. E.; Roots, C. M.; Bull, K. R.; Jeelall, Y.; Horikawa, K.; Whittle, B.; Balakishnan, B.; Sjollema, G.; Bertram, E. M.; Mackay, F.; Rimmer, A. J.; Cornall, R. J.; Field, M. A.; Andrews, T. D.; Goodnow, C. C.; Enders, A. B cell survival, surface BCR and BAFFR expression, CD74 metabolism, and CD8− dendritic cells require the intramembrane endopeptidase SPPL2A. *J. Exp. Med.* **2013**, *210*, 31−40.

(8) Schneppenheim, J.; Dressel, R.; Hüttl, S.; Lüllmann-Rauch, R.; Engelke, M.; Dittmann, K.; Wienands, J.; Eskelinen, E. L.; Hermans-Borgmeyer, I.; Fluhrer, R.; Saftig, P.; Schröder, B. The intramembrane protease SPPL2a promotes B cell development and controls endosomal traffic by cleavage of the invariant chain. *J. Exp. Med.* **2013**, *210*, 41−58.

(9) Kong, X.-F.; Martinez-Barricarte, R.; Kennedy, J.; Mele, F.; Lazarov, T.; Deenick, E. K.; Ma, C. S.; Breton, G.; Lucero, K. B.; Langlais, D.; Bousfiha, A.; Aytekin, C.; Markle, J.; Trouillet, C.; Jabot-Hanin, F.; Arlehamn, C. S. L.; Rao, G.; Picard, C.; Lasseau, T.; Latorre, D.; Hambleton, S.; Deswarte, C.; Itan, Y.; Abarca, K.; Moraes-Vasconcelos, D.; Ailal, F.; Ikincioglullari, A.; Dogu, F.; Benhsaien, I.; Sette, A.; Abel, L.; Boisson-Dupuis, S.; Schröder, B.; Nussenzweig, M. C.; Liu, K.; Geissmann, F.; Tangye, S. G.; Gros, P.; Sallusto, F.; Bustamante, J.; Casanova, J.-L. Disruption of an antimycobacterial circuit between dendritic and helper T cells in human SPPL2a deficiency. *Nat. Immunol.* **2018**, *19*, 973−985.

(10) Voss, M.; Schröder, B.; Fluhrer, R. Mechanism, specificity, and physiology of signal peptide peptidase (SPP) and SPP-like proteases. *Biochim. Biophys. Acta, Biomembr.* **2013**, *1828*, 2828−2839.

(11) Schröder, B. The multifaceted roles of the invariant chain CD74 - more than just a chaperone. *Biochim. Biophys. Acta, Mol. Cell Res.* **2016**, *1863*, 1269−1281.

(12) Niiro, H.; Clark, E. A. Regulation of B-cell fate by antigen-receptor signals. *Nat. Rev. Immunol.* **2002**, *2*, 945−956.

(13) Hüttl, S.; Kläsener, K.; Schweizer, M.; Schneppenheim, J.; Oberg, H.-H.; Kabelitz, D.; Reth, M.; Saftig, P.; Schröder, B. Processing of CD74 by the intramembrane protease SPPL2a is critical for B cell receptor signaling in transitional B cells. *J. Immunol.* **2015**, *195*, 1548−1563.

(14) Velcicky, J.; Bodendorf, U.; Rigollier, P.; Epple, R.; Beisner, D. R.; Guerini, D.; Smith, P.; Liu, B.; Feifel, R.; Wipfli, P.; Aichholz, R.; Couttet, P.; Dix, I.; Widmer, T.; Wen, B.; Brandl, T. Discovery of the first potent, selective, and orally bioavailable Signal Peptide Peptidase-Like 2a (SPPL2a) inhibitor displaying pronounced immunomodulatory effects in vivo. *J. Med. Chem.* **2018**, *61*, 865−880.

(15) Zhang, X.; Götte, M.; Ibig-Rehm, Y.; Schuffenhauer, A.; Kamke, M.; Beisner, D.; Guerini, D.; Siebert, D.; Bonamy, G. M. C.; Gabriel, D.; Bodendorf, U. Identification of SPPL2a inhibitors by multiparametric analysis of a high-content ultra-high-throughput screen. *SLAS Discov* **2017**, *22*, 1106−1119.

(16) Ghosh, A. K.; Osswald, H. L.; Prato, G. Recent progress in the development of HIV-1 protease inhibitors for the treatment of HIV/AIDS. *J. Med. Chem.* **2016**, *59*, 5172−5208.

(17) Eder, J.; Hommel, U.; Cumin, F.; Martoglio, B.; Gerhartz, B. Aspartic proteases in drug discovery. *Curr. Pharm. Des.* **2007**, *13*, 271−285.

(18) Ghosh, A. K.; Osswald, H. L. BACE1 (β-secretase) inhibitors for the treatment of Alzheimer's disease. *Chem. Soc. Rev.* **2014**, *43*, 6765−6813.

(19) McConnell, R. M.; Green, A. W.; Trana, C. J.; McConnell, M. S.; Lindley, J. F.; Sayyar, K.; Godwin, W. E.; Hatfield, S. E. New CathepsinD inhibitors with hydroxyethylamine isosteres: preparation and characterization. *Med. Chem.* **2006**, *2*, 27−38.

(20) Nöteberg, D.; Hamelink, E.; Hultén, J.; Wahlgren, M.; Vrang, L.; Samuelsson, B.; Hallberg, A. Design and synthesis of plasmepsin i and plasmepsin ii inhibitors with activity in plasmodium falciparum-infected cultured human erythrocytes. *J. Med. Chem.* **2003**, *46*, 734−746.

(21) Avdeef, A.; Berger, C. M.; Brownell, C. pH-Metric Solubility. 2: Correlation between the acid-base titration and the saturation shakeflask solubility-pH methods. *Pharm. Res.* **2000**, *17*, 85−89.

(22) Barnes-Seeman, D.; Jain, M.; Bell, L.; Ferreira, S.; Cohen, S.; Chen, X.-H.; Amin, J.; Snodgrass, B.; Hatsis, P. Metabolically stable tert-butyl replacement. *ACS Med. Chem. Lett.* **2013**, *4*, 514−516.

(23) Thompson, A. M.; Sutherland, H. S.; Palmer, B. D.; Kmentova, I.; Blaser, A.; Franzblau, S. G.; Wan, B.; Wang, Y.; Ma, Z.; Denny, W. A. Synthesis and structure activity relationships of varied ether linker analogues of the antitubercular drug (6*S*)-2-Nitro-6-{[4-(trifluoromethoxy)benzyl]oxy}-6,7-dihydro-5H-imidazo-[2,1-*b*][1,3]-oxazine (PA-824). *J. Med. Chem.* **2011**, *54*, 6563−6585.

(24) Cherian, S. K.; Kumar, P. Enantioselective synthesis of (+)-L-733,060. *Tetrahedron: Asymmetry* **2007**, *18*, 982−987.

(25) Wang, H.; Matsuhashi, H.; Doan, B. D.; Goodman, S. N.; Ouyang, X.; Clark, W. M., Jr. Large-scale synthesis of SB-462795, a cathepsin K inhibitor: the RCM-based approaches. *Tetrahedron* **2009**, *65*, 6291−6303.

DOI: 10.1021/acsmedchemlett.9b00044
ACS Med. Chem. Lett. XXXX, XXX, XXX−XXX

(26) Castejón, P.; Pastó, M.; Moyano, A.; Pericàs, M. A.; Riera, A. A convenient, stereodivergent approach to the enantioselective synthesis of *N*-Boc-aminoalkyl epoxides. *Tetrahedron Lett.* **1995**, *36*, 3019−3022.
(27) Ghosh, A. K.; Fidanze, S. Transition-state mimetics for HIV protease inhibitors: stereocontrolled synthesis of hydroxyethylene and hydroxyethylamine isosteres by ester-derived titanium enolate syn and anti-aldol reactions. *J. Org. Chem.* **1998**, *63*, 6146−6152.

DOI: 10.1021/acsmedchemlett.9b00044
ACS Med. Chem. Lett. XXXX, XXX, XXX−XXX